Anal Bioanal Chem
DOI 10.1007/s00216-016-9667-9

RESEARCH PAPER

Lectin binding studies on a glycopolymer brush flow-through biosensor by localized surface plasmon resonance

Ruben R. Rosencrantz[1,2] · Vu Hoa Nguyen[3] · Hyunji Park[4] · Christine Schulte[2] · Alexander Böker[4,5] · Uwe Schnakenberg[3] · Lothar Elling[1]

Received: 15 January 2016 / Revised: 20 May 2016 / Accepted: 25 May 2016

Abstract A localized surface plasmon resonance biosensor in a flow-through configuration was applied for investigating kinetics of lectin binding to surface-grafted glycopolymer brushes. Polycarbonate filter membranes with pore sizes of 400 nm were coated with a 114-nm thick gold layer and used as substrate for surface-initiated atom-transfer radical polymerization of a glycomonomer. These grafted from glycopolymer brushes were further modified with two subsequent enzymatic reactions on the surface to yield an immobilized trisaccharide presenting brush. Specific binding of lectins including *Clostridium difficile* toxin A receptor domain to the glycopolymer brush surface could be investigated in a microfluidic setup with flow-through of the analytes and transmission surface plasmon resonance spectroscopy.

Keywords Localized surface plasmon resonance · Glycopolymer brush · Microfluidics · Bacterial toxin · Glycosyltransferase · Biosensors

Ruben R. Rosencrantz, Vu Hoa Nguyen and Hyunji Park contributed equally to this work.

Electronic supplementary material The online version of this article (doi:10.1007/s00216-016-9667-9) contains supplementary material, which is available to authorized users.

✉ Lothar Elling
l.elling@biotec.rwth-aachen.de

[1] Laboratory for Biomaterials, Institute for Biotechnology and Helmholtz-Institute for Biomedical Engineering, RWTH Aachen University, Pauwelsstr. 20, 52074 Aachen, Germany

[2] Present address: Fraunhofer Institute for Applied Polymer Research, Geiselbergstraße 69, 14476 Potsdam, Germany

[3] Institute of Materials in Electrical Engineering 1, RWTH Aachen University, Sommerfeldstr. 24, 52074 Aachen, Germany

[4] Leibniz Institute for Interactive Materials, Department for Macromolecular Materials and Surfaces at RWTH Aachen, Forckenbeckstr. 50, 52074 Aachen, Germany

[5] Present address: Chair of Polymer Materials and Polymer Technologies, University of Potsdam, Fraunhofer Institute for Applied Polymer Research, Geiselbergstraße 69, 14476 Potsdam, Germany

Introduction

Among various optical sensing techniques, surface plasmon resonance (SPR) spectroscopy is until today the most widespread and standard analysis method for sensing biomolecular interactions and kinetics thereof. SPR displays excellent sensitivity in label-free real-time monitoring of refractive index changes in the vicinity of a sensor surface of a thin metal layer (commonly used gold surface with ~50 nm thickness) with plasmonic properties. The widely used Kretschmann configuration (reflection mode) requires a complex heavy-weight bulky measurement setup with a large sensor surface area [1]. The approach of localized surface plasmon resonance (LSPR) is the coupling of light with nanostructured objects, e.g., holes of a few hundred nanometers in diameter (subwavelength apertures) in either regular arrays or non-periodic short-range order patterns [2–8] or periodic grating structures [9, 10]. At these apertures, localized surface plasmons are excited normally by incident light in collinear optical geometry, called extraordinary light transmission (EOT) effect [3, 8]. The excitations in hole-type nanoapertures are observed as peaks in the spectral plot of the transmission signal.

The LSPR approach allows simplified transmission measurements at small sensor area footprints compared to complex measurements necessary to detect the reflection angle shifts in Kretschmann configurations [11]. These nanoplasmonic sensors are distinctive among photonic

Published online: 08 June 2016

sensors as they allow direct coupling of perpendicularly incident light and constitute a robust sensing platform minimizing the alignment requirements for light coupling [8]. The transmission setup is therefore more suitable for miniaturization.

Perforation of the gold layer and the underlying substrate in a LSPR device forces the analyte to flow through the active gold layer [8, 12]. In such a flow-through configuration, the analyte flow has to split up into a large number of sub-micron flow channels. This reduces significantly the transport limitation of conventional flow-over configurations and leads to an increased mass transport efficiency to the surface, decreased response times, and significant increased sensitivities [13–15]. We recently introduced an easy-to-use LSPR flow-through setup with a custom-made microfluidic chip which includes an exchangeable low-cost perforated polycarbonate filter membrane as sensor area [16].

(L)SPR is particularly useful for investigating the interactions between glycans and lectins, which describe the large class of carbohydrate binding proteins [17–20]. Glycans are intriguing complex biomolecules known for their high information coding capacity [21]. Due to their chemical variability based on multiple functional hydroxyl-groups and conformational diversity, they are involved in numerous biological tasks like cell communication, cell interactions, virus binding, cancer progression, and bacterial toxin evasion. Synthesis of complex glycans and revealing of glycan-protein interactions are still challenging aspects of glycoscience. Therefore, elucidation of structure relationships of glycans binding to lectins will support efforts to find glycan-based theranostic drugs for curing cancer or overcoming infections by pathogenic bacteria. SPR gave new insights to understand new aspects in binding behavior of lectins [17]. An important term in this regard is the "cluster glycoside effect," which describes the increase in affinity of lectins toward their glycoligand in orders of magnitude as soon as the number of presented glycans is increased fulfilling structural criteria to bind to the lectin [22]. This so-called multivalent effect is the basis of creating strong and specific glycan-protein interactions. We recently reported on the multivalent characteristics of glycopolymer brushes with good anti-fouling properties meaning very low unspecific protein adsorption [23]. The glycopolymer brushes display high specificity and selectivity for lectins depending on the presented glycan.

Encouraged by these results, we present here the lable-free kinetic analysis of lectin binding by LSPR. In detail, surface-initiated atom-transfer radical polymerization (SI-ATRP) for the synthesis of glycopolymer brushes grafted from the gold surface of the sensor foil was established for subsequent analysis of lectin binding by LSPR. At this stage, *N*-acetylglucosamine (GlcNAc) was presented on the brushes and the binding to this ligand was evaluated with the plant lectin *Griffonia simplicifolia* lectin II (GS-II), which is known to recognize specifically GlcNAc [24]. To get more variability on the ligand side, we applied a two-step enzymatic synthesis utilizing recombinant human and murine glycosyltransferases transferring two galactose (Gal) molecules to yield the trisaccharide Galα1,3Galβ1,4GlcNAcR, known as Galili-structure [25, 26]. This glycan epitope is reported to be a good ligand for the bacterial enterotoxin A (TcdA) from *Clostridium difficile* [27]. We investigated binding of the recombinantly expressed lectin domain (TcdA-R) of TcdA to Galili-structure and GlcNAc presenting brushes. A combination of SPR or electrochemical impedance spectroscopy (EIS) with surface-grafted polymer brushes as well as self-assembled monolayers (SAMS) was investigated previously and proved the high binding affinity of a lectin toward the glycopolymers with K_D values in the nanomolar range [28–30]. In contrast, we present here a novel method that combines a more cost-effective, disposable measuring platform with the versatility gained by multiple enzymatic reactions on the surface.

Experimental

For the flow-through LSPR measurements, the microfluidic chamber described in [16] was miniaturized to a cross-sectional area of 1.75 mm^2 and a volume of approximately 0.15 μl using standard PDMS soft-lithography technique in combination with photoresist (SU-8)-based micromolds. The chamber was connected to a fluid distribution system also made by soft-lithography technique which includes four inlet channels in PDMS with integrated micro-pneumatically driven micro valves [31]. The fluids were pressure-driven by 1-ml syringes and syringe pumps, which were controlled by a LabView program in order to automatize experiments with multiple rinsing steps. Teflon tubes were used with an inner diameter of 0.3 mm and an outer diameter of 0.76 mm to connect the devices. For all experiments, the flow rate was adjusted to 0.25 ml h^{-1} to obtain a good resolution of the adsorption process and to prevent mechanical deformations of the sensing membrane. Compared to the previously described macro reaction chamber [16], the actual volume of the miniaturized version was reduced by a factor of 30 and possesses a dead volume of only 2 μl. Hence, the lag time for medium exchange has been significantly reduced to less than 3 min instead of 20 min (Fig. 1). The overall recovery time of the modified device was determined by the bulk refractive index change during a consecutive exchange of sodium chloride (232 g l^{-1}) and de-ionized water (Fig. 1). The recovering time after a complete exchange could be reduced to 10 min compared to 54 min for the original macro chamber type. Thus, the additional miniaturization of the microfluidic system enables faster reaction times and lower analyte consumption.

The perforated polycarbonate membrane-based LSPR sensor was fabricated as previously reported [16]. Slight modifications refer to the polycarbonate filter with a pore diameter of

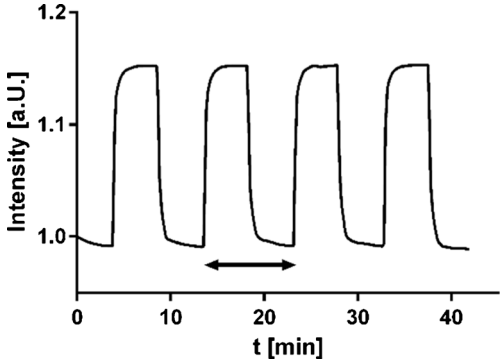

Fig. 1 Bulk refractive index measurement change during a consecutive exchange of sodium chloride and de-ionized water to determine the recovering time. The *double arrow* represents a time span of 10 min. NaCl solution of 20 μL and water were used for each injection, respectively

400 nm double-side coating with 114-nm-thick gold layers using a sputtering machine. For transmission measurements, the prepared foil is clamped into the reaction chamber to force a media flow through the nanopores (Fig. 2).

The complete microfluidic system was implemented into an optical bench consisting of a halogen lamp serving as light source and a spectrometer measuring the light transmission. Optical lenses were used to focus the light (Fig. 2). The transmitted light intensity was used to characterize the biomolecular interactions at the nanoaperture and for kinetic sensing. During an experiment, the averaged spectrum of ten individual measurements was stored in intervals of 10 s. The measurements were monitored by evaluating the intensity of the wavelength barycenter of the transmission spectra over the course of the experiment, according to [16]. The detailed experimental procedure and fabrication process of the microfluidic devices are described in the electronic supplementary material (ESM 1).

SI-ATRP was carried out on the sputtered membranes after deposition of the initiator bis[2-(2′-bromoisobutyryloxy)ethyl]disulfide (**1**) at room temperature using GlcNAc-2-hydroxyethylmethacrylate (GEMA) (**2**) as monomer in the presence of CuCl, $CuBr_2$, and bipyridine in a mixture of methanol/water (Fig. 3). In this way, we gained densely grafted glycopolymer brushes on the gold surface.

The surfaces were analyzed via atomic force microscopy (AFM) and scanning electron microscopy (SEM). The growth of the brush could be measured with AFM at high magnification, shown in Fig. 4a, b. However, the image gave some distortion due to the irregularity of the gold deposition and the roughness of the foil. A better view of the surface could be achieved by SEM, which clearly showed that the pores are not blocked after polymerization (Fig. 4c, d).

To prove the attachment of the glycopolymer brushes qualitatively, we performed fluorescence microscopy of the foils after incubating them with fluorescein isothiocyanate (FITC)-labeled GS-II as GlcNAc-binding lectin. A clear fluorescence signal was detected giving a hint that lectins do bind to this surface (Fig. 5). Next, we elongated GlcNAc on the surface with recombinantly expressed human β1,4-galactosyltransferase-1 (β4GalT) to yield *N*-acetyllactosamine (LacNAc) (3). This compound was used as an intermediate to perform a second enzymatic reaction using recombinant α1,3-galactosyltransferase (α3GalT) originating from mouse yielding the final Galili-epitope (4). The three surface-bound glycans were analyzed by FITC-GS-II and green fluorescent protein (eGFP)-labeled TcdA-R. The latter, as well as the non-labeled version of it, was expressed with an N-terminal His_6-Tag recombinantly in *Escherichia coli* BL21(DE3) pLysS. Whereas GS-II shows increased fluorescence signal on GlcNAc, it did not bind at all to Galili-structure. In contrast, TcdA-R showed signal on Galili-structure but did not bind to GlcNAc-presenting brushes (Fig. 5). The results of the specific lectin binding experiments indicated the attachment of glycopolymer brushes to the gold surface qualitatively. We additionally proved the successful SI-ATRP with glycomonomer by surface FTIR. The results are shown in the ESM. It is worth mentioning that all fluorescence measurements were carried out without any further blocking steps of the surface. This leads to the conclusion that the very good anti-fouling properties of the glycopolymer brushes which we observed on silicon surfaces [23] are maintained also on gold surfaces, and furthermore, glycan-specific binding of lectins is achieved also on the perforated gold foil.

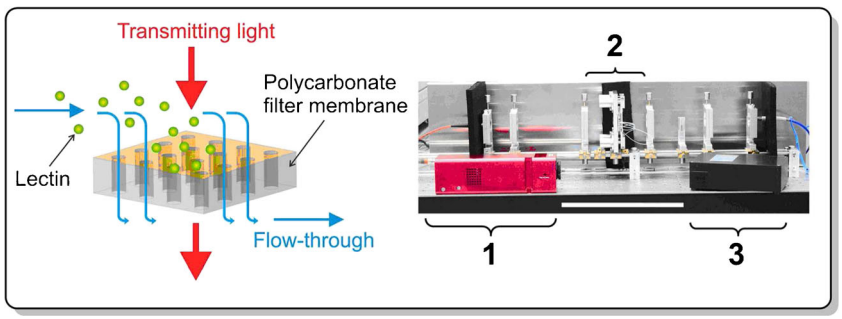

Fig. 2 Measuring setup of the flow-through LSPR biosensor and picture of the actual device. *1*: halogen lamp, *2*: sensor and microfluidic chamber, *3*: photodetector. *Scale bar* 20 cm

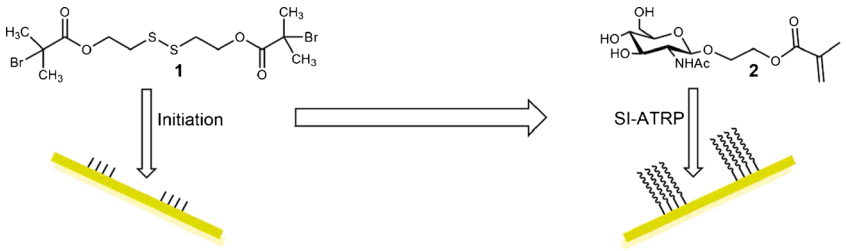

Fig. 3 General scheme of the polymerization process with SAM formation of the initiator **1** on the gold surface followed by SI-ATRP with glycomonomer **2**

Results and discussion

For adsorption analysis, we used low protein concentrations of 166.0 nM of GS-II and 155.0 nM of TcdA-R to get sufficient measuring signals, shown in Fig. 6. This sensitivity is slightly lower, yet in the same order of magnitude, than the sensitivity of commercially available SPR devices using Kretschmann configuration [32]. Thus, sensitivity in nanomolar range is still useful for both medical diagnostics as well as analytical purposes. The specificity of the LSPR device could be proven by binding studies of GS-II and TcdA-R to GlcNAc- and Galili-presenting glycobrushes, respectively (Fig. 6). Only very low unspecific binding to the sensor is observed (Fig. 6b, d). In fact, the specific binding signals increase by an 8-fold on Galili-glycopolymer brush sensors compared to GlcNAc for TcdA-R (Fig. 6c, d). For GS-II, the binding signal is 12-fold higher for GlcNAc-compared to Galili-structure presenting brushes (Fig. 6a, b). The range of unspecific adsorption of GS-II is about 7 % and of TcdA-R about 10 %. This means that 10 or 7 % of total binding signal has to be considered unspecific adsorption.

To gain insight into the kinetic parameters, we calculated k_{on}, k_{off}, and K_D from the sensorgrams (Table 1). We utilized a well-established binding model for biomolecular interactions based on first-order Langmuir kinetics. This model is valid for experiments without mass-transport limitation and is the most common model for SPR experiments, which are carried out under flow conditions [33–37]. As we force the flow though the pores with very small cross section, limitation by diffusion is unlikely. Additionally, the whole flow cell volume is very small, again making mass transfer limitation not expectable. Therefore, we used for fitting the association part of the measured curves, Eq. (1) [38].

$$c_{\text{lectin}}(t) = \frac{B_{\max} \times c_0}{c_0 + K_D} \times 1 - e^{-(k_{\text{on}} + k_{\text{off}}) \times t} \quad (1)$$

with $B_{\max}$ as maximal load of surface with lectin and c_0 as initial concentration of lectin. For fitting the dissociation process, we used Eq. (2) [39], which adds a term for dissociation after t_0. t_0 is the time point of dissociation initiation.

$$c_{\text{lectin}}(t) = \frac{B_{\max} \times c_0}{c_0 + K_D} \times 1 - e^{-(k_{\text{on}} + k_{\text{off}}) \times t_0} \times e^{-k_{\text{off}} \times (t - t_0)} \quad (2)$$

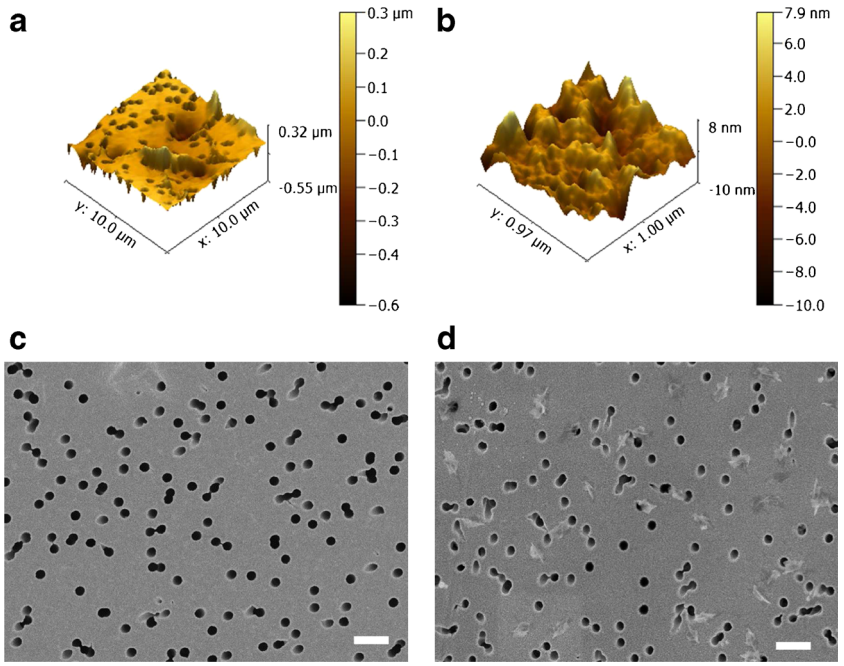

Fig. 4 AFM and SEM images of **A**, **C** untreated gold covered foil and **B**, **D** foil after SI-ATRP with glycopolymer brushes. *Scale bars* in SEM images represent 1 µm. As indicated by the AFM analysis, the polymerization increases surface roughness and the nanopores are not detected anymore (**B**) by measurements at the nanometer level. However, with SEM, it is clearly shown that the pores (*black*) are free and not blocked by polymer (**D**), which leads to the conclusion that the polymer will not affect the flow-through setup. For SEM analysis, the foil was sputtered with platinum prior to measurement

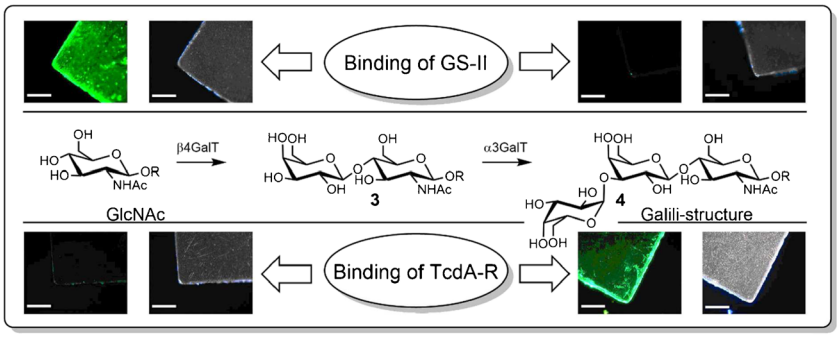

Fig. 5 Enzymatic synthesis with respective fluorescence lectin analysis (*green*) and dark field images of the foils. GS-II clearly binds to GlcNAc, whereas no fluorescence is detected on Galili-structure. In contrast, TcdA-R binds to Galili-structure, but not to GlcNAc. The dark field images of the foils are used for clarification of the foil location in fluorescence pictures. *Scale bars* 100 μm

Using Eqs. (1) and (2), we were able to determine the kinetic parameters of lectin binding to the brushes on the foil, by taking association as well as dissociation by dilution into account. This circumvents the necessity of measuring different protein concentrations for determination of K_D. Interestingly, the used model describes one-to-one binding modes but still gives convenient results with lectin-glycan interactions, although lectins are assumed to have multiple binding sites. Therefore, interactions between glycans and lectins may be considered as one-to-one interactions in this study. The multivalent presentation of the glycans increases the affinity of the lectins in orders of magnitude and reveals low nanomolar K_D values. These results confirm our previous studies on GS-II binding on GlcNAc-glycopolymer brushes by EIS [30]. This additional data with commercially available lectin validates the general applicability of glycopolymer brushes as high-affinity multivalent scaffolds for lectin analysis. The superb binding properties of multivalent glycopolymer brushes were further proven also by inhibition experiments high IC_{50} values for the corresponding glycan ligands in solution [23, 28, 40]. In contrast, studying ligands with less multivalency K_D values in the lower μM range are commonly found for lectins [41, 42]. Most importantly, the receptor binding domain of toxin A from *C. difficile* (TcdA-R) binds also with K_D values of low nanomole concentrations to Galili-epitope-presenting glycopolymer brushes (Table 1). To the best of our knowledge, this is the first time that kinetic data of TcdA-R binding to carbohydrate structures like Galili-structure in a multivalent environment was elucidated. It must be taken into consideration that TcdA-R consists of up to seven putative binding sites; therefore, the one-to-one model may not be the best representation. Nevertheless, the experimental data are well described by this simple model (see ESM). Binding to soluble glycans revealed weak

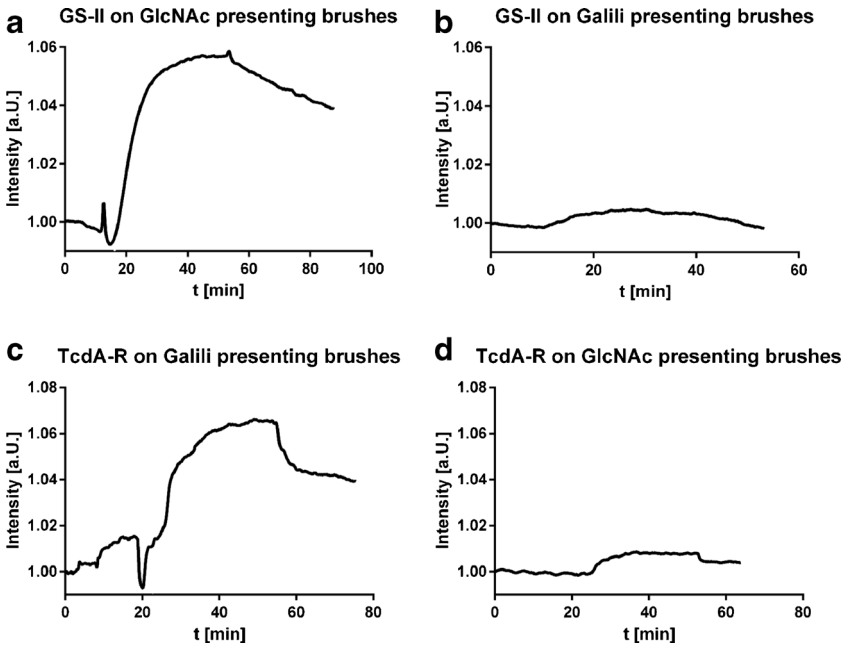

Fig. 6 LSPR sensorgrams for binding of GS-II to GlcNAc presenting brushes (**A**) and Galili (**B**) as negative control. **C**, **D** represent the binding cruves of TcdaA-R to Galili-structure and GlcNAc as negative control, respectively. The measurements were carried out as triplicates. For complete data, see ESM

Table 1 Kinetic parameters collected by LSPR for GS-II binding to GlcNAc presenting brushes and TcdA-R binding to Galili-epitope

	k_{on} [M^{-1} s^{-1}]	k_{off} [s^{-1}]	K_D [M]
GS-II	$5.4 \times 10^5 \pm 3.0 \times 10^5$	$1.3 \times 10^{-3} \pm 4.1 \times 10^{-4}$	$4.2 \times 10^{-9} \pm 3.5 \times 10^{-9}$
TcdA-R	$2.2 \times 10^6 \pm 1.0 \times 10^6$	$5.5 \times 10^{-4} \pm 2.2 \times 10^{-4}$	$3.0 \times 10^{-10} \pm 1.9 \times 10^{-10}$

association of TcdA due to the lack of multivalent presentation and K_D values were set at the range of 0.5 mM [43, 44]. For this lectin, multivalent presentation may be especially important and favorable, as the receptor domain bears approximately seven potential carbohydrate recognition domains (CRDs) [45]. Due to flexibility of the brushes and the high number of glycans in close proximity to each other, individual CRDs may choose the optimal adjacent glycan ligand for binding. This results here in K_D values in the low nanomolar range. The strong multivalent interactions between glycan-ligand and lectin lead to high-affinity binding with K_D values similar to antibody-antigen interactions [46]. This is a unique feature of the glycan presentation by surface-mounted glycopolymer brushes. It is well described that the binding strength of lectin to carbohydrates increases in orders of magnitude as soon as the ligand is presented in a multivalent manner. This effect is called the "cluster glycoside effect" and explained for example by ligand chelation with lectins bearing multiple binding sites [22]. The topology of the glycopolymer brushes provides a multivalent environment in all directions of space: perpendicular to the sensor surface given by the degree of polymerization, which is directly related to the numbers of presented glycans and in-plane of the sensor surface by dense grafting (see ESM). Taking the k_{off} values in consideration, approximate half-lives of the lectin-carbohydrate complexes were determined with values of about 30 h for TcdA-R and about 10 h for GS-II. Half-lives in this range are important indicators for the development of novel carbohydrate-based scavengers of bacterial toxins. The rather low sample amount needed in our approach renders these sensors as versatile disposable diagnostic device for monitoring infections with *C. difficile* by measuring the abundancy of TcdA. Not only high-affinity ligands are created but also the sensitivity of LSPR is in a suitable range, as clinically used assays detect 2.5 ng mL^{-1} and higher in stool [47]. Generally, 50 mg of sample is used in commercially available α-TcdA ELISAs, this would also be sufficient for our device, while omitting the time-consuming multi-step ELISA procedure. Normally, k_{on} is determined by the rate of diffusion and is found in ranges of 10^6–10^8 M^{-1} s^{-1}. Both lectins show values of 10^5–10^6 M^{-1} s^{-1} not uncommon for biomolecular interactions. In this case, overall slower binding may be additionally caused by the multiple binding sites in both lectins. GS-II consists of two or four binding sites depending if it is originated from leaves or seeds, whereas TcdA-R shows up to seven CRDs [48]. This causes a slower binding of the lectins in general depending on how much binding sites are tackled at once. Comparison of these findings with other lectins reveals that rather slow binding is common for these proteins, even if high-affinity ligands are presented [42, 49, 50].

Compared with other methods which are used for detecting lectin interactions like EIS [30], conventional SPR [17], quartz crystal microbalance (QCM) [51], or isothermal titration calorimetry (ITC) [52], our LSPR is similar in sensitivity and offers the advantages of disposability and cost-effectiveness. The low-cost production of the foil-based biosensors is straightforward compared to commonly used gold-coated glass chips in the SPR Kretschmann configuration [53]. Moreover, sample sizes are small when using our new LSPR approach. Although in comparison to ITC, not all the thermodynamic parameters may be monitored, SPR measurements by our device fulfill the task of determining binding kinetics of biomolecular interactions with high satisfaction.

Conclusion

The developed microfluidic flow-through LSPR setup leads to a reduced sensor area and consumption of fluid volumes compared to commonly used SPR Kretschmann configurations. This setup gives valid information about lectin binding to glycopolymer-brush surfaces. We were able to synthesize complex glycan-structures on the sensor surfaces utilizing recombinant glycosyltransferases. Glycan-specific binding of a plant lectin and a recombinantly expressed bacterial enterotoxin binding domain was proven and analyzed to gain insight into binding kinetics. The measurement setup is variable with respect to presented ligands and represents an economic and disposable LSPR setup for measuring protein-ligand interactions. In combination with our high-affinity glycan-ligands, this platform is ideally configured for future fast and specific diagnostics of TcdA-mediated infections. Our system is optimized for lectin binding with a very multivalent surface covering resulting in high-affinity binding of lectins with K_D values common for antibody-antigen interaction. Simultaneously, our system shows very low unspecific adhesion of lectins, which is also superior to commercially available SPR chip functionalization with hydrogels or dextrane. This enables the use as diagnostic glycan-based device to detect low amounts of bacterial enterotoxins or other disease-relevant lectins. In comparison to commercial

Kretschmann configuration SPR instruments, the LSPR approach we took is 95 % cheaper and may be miniaturized, with still reasonable sensitivity, which allows the use of this device in the field or by standard diagnostic laboratories. Broadening the scope of this system to other glycan epitopes is easily achieved by performing different enzymatic reactions on the surface, giving a high-affinity, low-fouling, yet low-cost and disposable measuring device, with variable ligand presentation for binding analysis of lectins. In general, the developed sensor may be used for any kind of investigations of kinetics of biomolecule interactions.

Acknowledgments R.R.R., L.E., and A.B. acknowledge funding by the Deutsche Forschungsgemeinschaft (DFG) in the framework of the SFB 985.

Compliance with ethical standards The research did not involve human participants or animals.

Conflict of interest The authors declare that they have no conflict of interest.

References

1. Kretschmann E, Raether H. Radiative decay of non radiative surface plasmons excited by light. Z Naturforsch A. 1968;23:2135–6.
2. Cooper M. Label-free screening of bio-molecular interactions. Anal Bioanal Chem. 2003;377(5):834–42. doi:10.1007/s00216-003-2111-y.
3. Ebbesen TW, Lezec HJ, Ghaemi HF, Thio T, Wolff PA. Extraordinary optical transmission through sub-wavelength hole arrays. Nature. 1998;391(6668):667–9.
4. Escobedo C, Vincent S, Choudhury AIK, Campbell J, Brolo AG, Sinton D, et al. Integrated nanohole array surface plasmon resonance sensing device using a dual-wavelength source. J Micromech Microeng. 2011;21(11):115001.
5. Estevez MC, Otte MA, Sepulveda B, Lechuga LM. Trends and challenges of refractometric nanoplasmonic biosensors: a review. Anal Chim Acta. 2014;806:55–73. doi:10.1016/j.aca.2013.10.048.
6. Ferreira J, Santos MJL, Rahman MM, Brolo AG, Gordon R, Sinton D, et al. Attomolar protein detection using in-hole surface plasmon resonance. J Am Chem Soc. 2009;131(2):436–7. doi:10.1021/ja807704v.
7. Jonsson MP, Dahlin AB, Feuz L, Petronis S, Höök F. Locally functionalized short-range ordered nanoplasmonic pores for bioanalytical sensing. Anal Chem. 2010;82(5):2087–94. doi:10.1021/ac902925e.
8. Yanik AA, Wang X, Erramilli S, Hong MK, Altug H. Extraordinary midinfrared transmission of rectangular coaxial nanoaperture arrays. Applied Physics Letters. 2008;93(8):081104. doi:10.1063/1.2973165.
9. Singh BK, Hillier AC. Surface plasmon resonance enhanced transmission of light through gold-coated diffraction gratings. Anal Chem. 2008;80(10):3803–10. doi:10.1021/ac800045a.
10. Yeh D-M, Huang C-F, Chen C-Y, Lu Y-C, Yang CC. Localized surface plasmon-induced emission enhancement of a green light-emitting diode. Nanotechnology. 2008;19(34):345201.
11. Brolo AG. Plasmonics for future biosensors. Nat Photon. 2012;6(11):709–13.
12. Eftekhari F, Escobedo C, Ferreira J, Duan X, Girotto EM, Brolo AG, et al. Nanoholes as nanochannels: flow-through plasmonic sensing. Anal Chem. 2009;81(11):4308–11. doi:10.1021/ac900221y.
13. Escobedo C, Brolo AG, Gordon R, Sinton D. Flow-through vs flow-over: analysis of transport and binding in nanohole array plasmonic biosensors. Anal Chem. 2010;82(24):10015–20. doi:10.1021/ac101654f.
14. Yanik AA, Huang M, Artar A, Chang T-Y, Altug H. Integrated nanoplasmonic-nanofluidic biosensors with targeted delivery of analytes. Appl Phys Lett. 2010;96(2):021101. doi:10.1063/1.3290633.
15. Yanik AA, Huang M, Kamohara O, Artar A, Geisbert TW, Connor JH, et al. An optofluidic nanoplasmonic biosensor for direct detection of live viruses from biological media. Nano Lett. 2010;10(12):4962–9. doi:10.1021/nl103025u.
16. Buchenauer A, Bialon M, Segun D, Püttmann C, Stein C, Barth S, et al. Plasmonic flow-through biosensor using a polymeric substrate. J Micromech Microeng. 2014;24(3):034001.
17. Duverger E, Frison N, Roche A-C, Monsigny M. Carbohydrate-lectin interactions assessed by surface plasmon resonance. Biochimie. 2003;85(1–2):167–79. doi:10.1016/S0300-9084(03)00060-9.
18. Karamanska R, Clarke J, Blixt O, MacRae J, Zhang J, Crocker P, et al. Surface plasmon resonance imaging for real-time, label-free analysis of protein interactions with carbohydrate microarrays. Glycoconj J. 2008;25(1):69–74. doi:10.1007/s10719-007-9047-y.
19. Smith EA, Thomas WD, Kiessling LL, Corn RM. Surface plasmon resonance imaging studies of protein-carbohydrate interactions. J Am Chem Soc. 2003;125(20):6140–8. doi:10.1021/ja034165u.
20. Zeng X, Andrade CS, Oliveira ML, Sun X-L. Carbohydrate–protein interactions and their biosensing applications. Anal Bioanal Chem. 2012;402(10):3161–76. doi:10.1007/s00216-011-5594-y.
21. Varki A. Biological roles of oligosaccharides: all of the theories are correct. Glycobiology. 1993;3(2):97–130.
22. Lundquist JJ, Toone EJ. The cluster glycoside effect. Chem Rev. 2002;102(2):555–78.
23. Park H, Rosencrantz RR, Elling L, Böker A. Glycopolymer brushes for specific lectin binding by controlled multivalent presentation of N-acetyllactosamine glycan oligomers. Macromol Rapid Commun. 2015;36(1):45–54. doi:10.1002/marc.201400453.
24. Zhu K, Bressan RA, Hasegawa PM, Murdock LL. Identification of N-acetylglucosamine binding residues in Griffonia simplicifolia lectin II. FEBS Lett. 1996;390(3):271–4.
25. Galili U. Immune response, accommodation, and tolerance to transplantation carbohydrate antigens. Transplantation. 2004;78(8):1093–8.
26. Kupper CE, Rosencrantz RR, Henssen B, Pelantova H, Thones S, Drozdova A, et al. Chemo-enzymatic modification of poly-N-acetyllactosamine (LacNAc) oligomers and N, N-diacetyllactosamine (LacDiNAc) based on galactose oxidase treatment. Beilstein J Org Chem. 2012;8:712–25. doi:10.3762/bjoc.8.80.
27. Ivarsson ME, Leroux J-C, Castagner B. Targeting bacterial toxins. Angew Chem Int Ed. 2012;51(17):4024–45. doi:10.1002/anie.201104384.
28. Meng X-L, Fang Y, Wan L-S, Huang X-J, Xu Z-K. Glycopolymer brushes for the affinity adsorption of RCA120: effects of thickness, grafting density, and epitope density. Langmuir. 2012;28(38):13616–23. doi:10.1021/la302389e.
29. Bhattarai JK, Sharma A, Fujikawa K, Demchenko AV, Stine KJ. Electrochemical synthesis of nanostructured gold film for the study of carbohydrate-lectin interactions using localized surface plasmon resonance spectroscopy. Carbohyd Res. 2015;405:55–65. doi:10.1016/j.carres.2014.08.019.
30. Lazar J, Park H, Rosencrantz RR, Böker A, Elling L, Schnakenberg U. Evaluating the thickness of multivalent glycopolymer brushes

for lectin binding. Macromol Rapid Commun. 2015;36(16):1472–8. doi:10.1002/marc.201500118.
31. Unger MA, Chou H-P, Thorsen T, Scherer A, Quake SR. Monolithic microfabricated valves and pumps by multilayer soft lithography. Science. 2000;288(5463):113–6. doi:10.1126/science.288.5463.113.
32. Choi S, Wang R, Lajevardi-Khosh A, Chae J. Using competitive protein adsorption to measure fibrinogen in undiluted human serum. Appl Phys Lett. 2010;97(25):253701. doi:10.1063/1.3529445.
33. Goodrich JA, Kugel JF. Binding and kinetics for molecular biologists. CSHL Press; 2007.
34. Chaiken I, Rose S, Karlsson R. Analysis of macromolecular interactions using immobilized ligands. Anal Biochem. 1992;201(2):197–210.
35. Gervais T, Jensen KF. Mass transport and surface reactions in microfluidic systems. Chem Eng Sci. 2006;61(4):1102–21.
36. Hahnefeld C, Drewianka S, Herberg FW. Determination of kinetic data using surface plasmon resonance biosensors. Methods Mol Med. 2004;94:299–320.
37. Drescher DG, Ramakrishnan NA, Drescher MJ. Surface plasmon resonance (SPR) analysis of binding interactions of proteins in inner-ear sensory epithelia. Methods Mol Biol (Clifton, NJ). 2009;493:323–43. doi:10.1007/978-1-59745-523-7_20.
38. Edwards PR, Maule CH, Leatherbarrow RJ, Winzor DJ. Second-order kinetic analysis of IAsys biosensor data: its use and applicability. Anal Biochem. 1998;263(1):1–12. doi:10.1006/abio.1998.2814.
39. de Mol NJ, Fischer MJE. Chapter 5 kinetic and thermodynamic analysis of ligand-receptor interactions: SPR applications in drug development. Handbook of surface plasmon resonance. Royal Soc Chem. 2008:123–72.
40. Goudot A, Pourceau G, Meyer A, Gehin T, Vidal S, Vasseur J-J, et al. Quantitative analysis (Kd and IC50) of glycoconjugates interactions with a bacterial lectin on a carbohydrate microarray with DNA direct immobilization (DDI). Biosens Bioelectron. 2013;40(1):153–60. doi:10.1016/j.bios.2012.07.003.
41. Rachel H, Chang-Chun L. Chapter 5—recent advances toward the development of inhibitors to attenuate tumor metastasis via the interruption of lectin-ligand interactions. In: Derek H, editor. Adv Carbohydr Chem Biochem. Academic Press; 2013. p. 125–207.
42. Dam TK, Cavada BS, Grangeiro TB, Santos CF, Ceccatto VM, de Sousa FAM, et al. Thermodynamic binding studies of lectins from the Diocleinae subtribe to deoxy analogs of the core trimannoside of asparagine-linked oligosaccharides. J Biol Chem. 2000;275(21):16119–26. doi:10.1074/jbc.M000670200.
43. El-Hawiet A, Kitova EN, Kitov PI, Eugenio L, Ng KK, Mulvey GL, et al. Binding of Clostridium difficile toxins to human milk oligosaccharides. Glycobiology. 2011;21(9):1217–27. doi:10.1093/glycob/cwr055.
44. Nguyen TT, Kim JW, Park JS, Hwang KH, Jang TS, Kim CH, et al. Identification of oligosaccharides in human milk bound onto the toxin A carbohydrate binding site of Clostridium difficile. J Microbiol Biotechnol. 2015. doi:10.4014/jmb.1509.09034.
45. Ho JGS, Greco A, Rupnik M, Ng KK-S. Crystal structure of receptor-binding C-terminal repeats from Clostridium difficile toxin A. Proc Natl Acad Sci U S A. 2005;102(51):18373–8. doi:10.1073/pnas.0506391102.
46. Hussack G, Arbabi-Ghahroudi M, van Faassen H, Songer JG, Ng KK-S, MacKenzie R, et al. Neutralization of Clostridium difficile toxin A with single-domain antibodies targeting the cell receptor binding domain. J Biol Chem. 2011;286(11):8961–76. doi:10.1074/jbc.M110.198754.
47. Song L, Zhao M, Duffy DC, Hansen J, Shields K, Wungjiranirun M, et al. Development and validation of digital enzyme-linked immunosorbent assays for ultrasensitive detection and quantification of Clostridium difficile toxins in stool. J Clin Microbiol. 2015;53(10):3204–12. doi:10.1128/jcm.01334-15.
48. Zhu-Salzman K, Shade RE, Koiwa H, Salzman RA, Narasimhan M, Bressan RA, et al. Carbohydrate binding and resistance to proteolysis control insecticidal activity of Griffonia simplicifolia lectin II. Proc Natl Acad Sci U S A. 1998;95(25):15123–8.
49. Cseh S, Vera L, Matsushita M, Fujita T, Arlaud GJ, Thielens NM. Characterization of the interaction between L-ficolin/p35 and mannan-binding lectin-associated serine proteases-1 and -2. J Immunol (Baltimore, Md : 1950). 2002;169(10):5735–43.
50. Teillet F, Dublet B, Andrieu J-P, Gaboriaud C, Arlaud GJ, Thielens NM. The two major oligomeric forms of human mannan-binding lectin: chemical characterization, carbohydrate-binding properties, and interaction with MBL-associated serine proteases. J Immunol. 2005;174(5):2870–7. doi:10.4049/jimmunol.174.5.2870.
51. Gou Y, Richards S-J, Haddleton DM, Gibson MI. Investigation of glycopolymer-lectin interactions using QCM-d: comparison of surface binding with inhibitory activity. Polym Chem. 2012;3(6):1634–40. doi:10.1039/C2PY20140B.
52. Wang Z, Chen G, Lu J, Hong L, Ngai T. Investigation of the factors affecting the carbohydrate-lectin interaction by ITC and QCM-D. Colloid Polym Sci. 2014;292(2):391–8. doi:10.1007/s00396-013-3080-0.
53. Tang Y, Zeng X, Liang J. Surface plasmon resonance: an introduction to a surface spectroscopy technique. J Chem Educ. 2010;87(7):742–6. doi:10.1021/ed100186y.